Ka-band Microwave Frequency Comb Doppler Reflectometer System for the Large Helical Device

Tokihiko TOKUZAWA, Shigeru INAGAKI[1)], Akira EJIRI[2)], Ryota SOGA[3)], Ichihiro YAMADA, Shin KUBO, Mikiro YOSHINUMA, Katsumi IDA, Chihiro SUZUKI, Kenji TANAKA, Tsuyoshi AKIYAMA, Naohiro KASUYA[1)], Kimitaka ITOH, Kiyomasa WATANABE, Hiroshi YAMADA, Kazuo KAWAHATA and LHD Experiment Group

National Institute for Fusion Science, 322-6 Oroshi-cho, Toki 509-5292, Japan
[1)]*Research Institute for Applied Mechanics, Kyushu University, Kasuga 816-8580, Japan*
[2)]*Graduate School of Frontier Sciences, The University of Tokyo, Kashiwa 277-8561, Japan*
[3)]*Department of Energy Engineering and Science, Nagoya University, Furo-cho, Chikusa-ku, Nagoya 464-8601, Japan*

(Received 9 July 2014 / Accepted 8 September 2014)

A *ka*-band multi-channel Doppler reflectometer system was constructed for the Large Helical Device (LHD) using a comb frequency generator as a source. A filter bank system is utilized for precise quadrature phase detection, and preliminary back-scattered waves were obtained in LHD plasma experiments. In addition, a direct digital signal acquisition system was successfully demonstrated for providing a greater number of multi-channel measurements.

Keywords: Doppler reflectometer, frequency comb, microwave, density fluctuation, poloidal velocity

DOI: 10.1585/pfr.9.1402149

1. Introduction

Doppler reflectometry (also called Doppler back-scattering: DBS) is a unique technique when used in combination with the back-scattering method, which provides a wavenumber resolution, and reflectometry, which provides a high-spatial resolution [1]. Doppler reflectometry can measure the perpendicular velocity of electron density fluctuations $v_\perp$, the radial electric field E_r, and the perpendicular wavenumber spectrum $S(k_\perp)$ in magnetized confinement plasmas. As a result, a number of systems have been used in worldwide fusion plasma devices, such as tokamaks (Tuman-3M [2], ASDEX Upgrade [3–5], Tore Supra [6, 7], DIII-D [8, 9], JT-60U [10]) and helical/stellarators (Wendelstein 7-AS [1, 11], TJ-II [12], LHD [13]).

Recently, a multi-channel system operating over a broad frequency range has been demonstrated [9]. The system is utilized for measuring not only the spatial structure of the plasma parameters, but also the temporal relationship between two (or many) points in space. These measurements are quite helpful for evaluating plasma turbulence, transport, and confinement phenomena. For these reasons, a new multi-channel Doppler reflectometer has been developed for the Large Helical Device (LHD).

From a technical point of view, this novel multi-channel system is based on the previous development of a high-frequency and low phase-noise frequency comb generator. A frequency comb itself is an influential modern technology, for applications such as an optical laser comb [14], terahertz comb [15], and others. The present development for fusion plasma diagnostics is recognized as one of the applications of the frequency comb technique. Figure 1 shows an example of the frequency spectrum of the comb generator output. Here, a modulation frequency of 410 MHz is applied to the comb generator. Numerous comb frequency components can be observed up to 20 GHz, and their separation is easily controlled by the modulator. When the comb generator output is launched to the plasma and the cut-off condition of each frequency is satisfied, each frequency component returns from its corresponding position. Therefore, a time resolved multi-point measurement, representing a spatio-temporal observation, has been made possible.

The principle of Doppler reflectometry is explained simply as follows. When a deliberately tilted probe wave beam is launched to a plasma, it is refracted according to the density gradient. As the wave propagates, the wavenumber decreases with the refractive index. When the wavenumber reaches a minimum, the beam is turned and reflected back. In addition, at the turning point, the wave is sensitive to fluctuations of the refractive index. If the fluctuation satisfies the Bragg condition, i.e., $\boldsymbol{k} = -2\boldsymbol{k}_\mathrm{i}$ (where $\boldsymbol{k}_\mathrm{i}$ is the local wave vector of the launching beam), the scattered radiation will be returned. In addition, when the fluctuations move with a velocity $\boldsymbol{v}$, the backscattered signal shows a Doppler frequency shift $\omega_\mathrm{D} = \boldsymbol{v} \cdot \boldsymbol{k} = v_\perp k_\perp + v_\parallel k_\parallel + v_\mathrm{r} k_\mathrm{r}$. Here, the subscripts $_\parallel$ and r indicate the

author's e-mail: tokuzawa@nifs.ac.jp

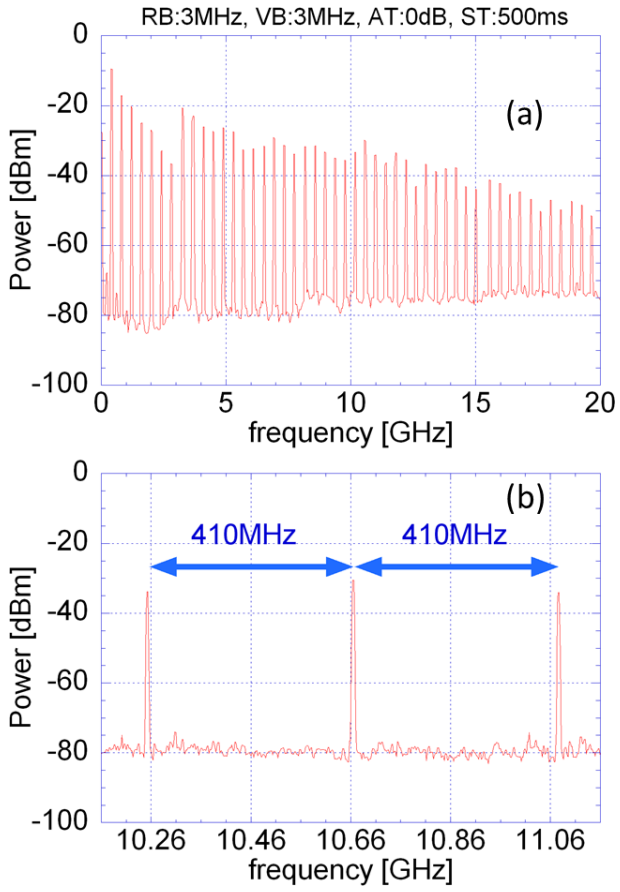

Fig. 1 Example of the frequency spectrum of the comb generator output. Here, the comb generator is operated with a 410 MHz stable source modulation. (a) The entire frequency range and (b) an enlarged view around 10.5 GHz.

parallel and radial directions, respectively. It can usually be assumed that $k_\perp \gg k_\parallel$ and $v_\perp < v_\parallel$, so that the second term ($v_\parallel k_\parallel$) is negligible in comparison with the first term ($v_\perp k_\perp$). If, in addition, the turbulence does not displace itself radially, the third term vanishes and $\omega_D \approx v_\perp k_\perp$. Then, the perpendicular velocity $v_\perp$ of the selected fluctuation can be calculated. The perpendicular velocity is a composition of the plasma background $\boldsymbol{E} \times \boldsymbol{B}$ velocity $v_{E\times B}$ and the intrinsic phase velocity of the density fluctuations v_{ph}, and this composition is given as $v_\perp = v_{\mathbf{E}\times\mathbf{B}} + v_{ph}$. If v_{ph} is known or $v_{ph} \ll v_{E\times B}$ (which is usually satisfied at the plasma edge in magnetically confined devices), the radial electric field E_r can be extracted from the measurement of the perpendicular velocity through $E_r = v_\perp B$, where B is the absolute value of the magnetic field [1,3,7].

In this paper, we describe the diagnostics system status in Sec. 2 and present an analysis of the system performance and preliminary experimental results in Sec. 3. The first trial conducted using direct signal acquisition is described in Sec. 4.

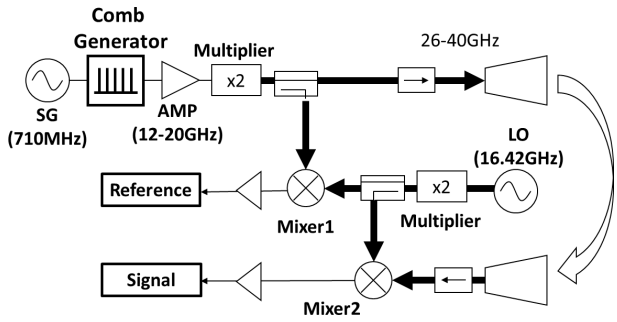

Fig. 2 Schematic of the *ka*-band microwave circuit for the Doppler reflectometer comprising a comb generator. A 710 MHz synthesized signal generator (SG) is used as a modulator. A 30 dB amplifier and an active multiplier provide the *ka*-band probe wave. A 16.42 GHz local oscillator (LO) is used for heterodyne detection. Two intermediatefrequency (IF) components, which are indicated as "Reference" and "Signal," are fed to the receiver section described in Fig. 3.

2. Diagnostics System Design

The *ka*-band microwave frequency comb Doppler reflectometer system is described as follows. The system comprises two sections that consist of a microwave circuit shown in Fig. 2 and a receiver section shown in Fig. 3. A passive, nonlinear transmission line (NLTL: PSPL model 7112) modulated by a stable synthesizer is used as the frequency comb source. NLTLs have excellent low phase noise performance [16,17] and generate an array of equally spaced (presently, $\Delta f = 0.71$ GHz) frequencies with a slow decay in output power. The frequency range of the output is initially up to 20 GHz. The wave is amplified in the frequency range of 12 - 20 GHz. The wave frequency is subsequently doubled followed by a frequency active multiplier in the *ka*-band (26 - 40 GHz). In the *ka*-band, the number of comb components is around 20 (i.e., 14 GHz/0.7 GHz). Therefore, 20 frequency components can be simultaneously launched to the plasma. The probe beam is launched and received by bistatic conical horn antennas with a lens, and these antennas can modify the launching angle to the plasma [18]. The antenna angle is slightly tilted toward the normal of the plasma surface in the horizontal cross section for Doppler reflectometry operation. The Doppler-shifted back-scattered signal is mixed with a local wave whose frequency is 32.84 GHz. Reduction of the frequency range of the intermediate frequency (IF) signal by tuning the local frequency was successfully achieved. The IF signal has several frequency comb components, as shown in Fig. 4. Comb frequency components less than 6 GHz are clearly observed. The IF signal, denoted as "Signal," is generated as shown in Fig. 2. A portion of the probe wave is divided and fed to mixer (Mixer 1) to form what is denoted as the "Reference" signal in Fig. 2 for heterodyne detection.

The down-converted IF signals are fed to a receiver

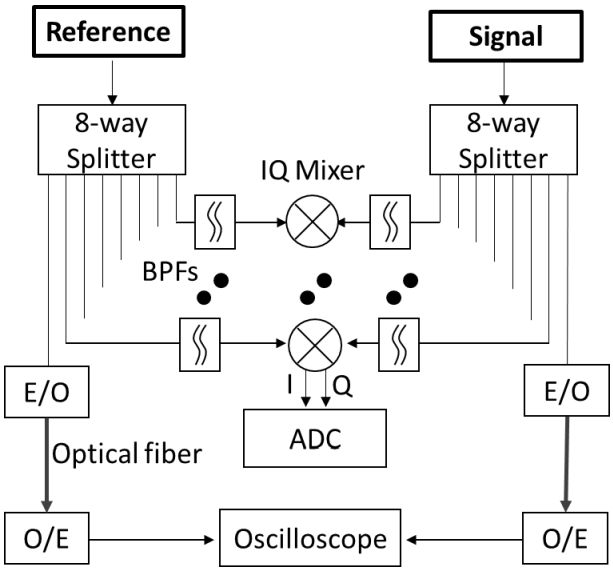

Fig. 3 Schematic of the receiver section. Each IF signal (Reference and Signal) is divided in to eight separate signals. The filter bank system comprises seven band pass filters (whose center frequencies are 0.53, 0.88, 1.95, 2.30, 3.70, 4.08, and 5.10 GHz) for quadrature signal detection. The output of IQ detection is fed to the 1 MHz data acquisition system (ADC). Also, a portion of the 8-way output is fed to an electro-optical converter set (E/O and O/E) and transmitted via an optical fiber directly to the diagnostic room for direct signal acquisition.

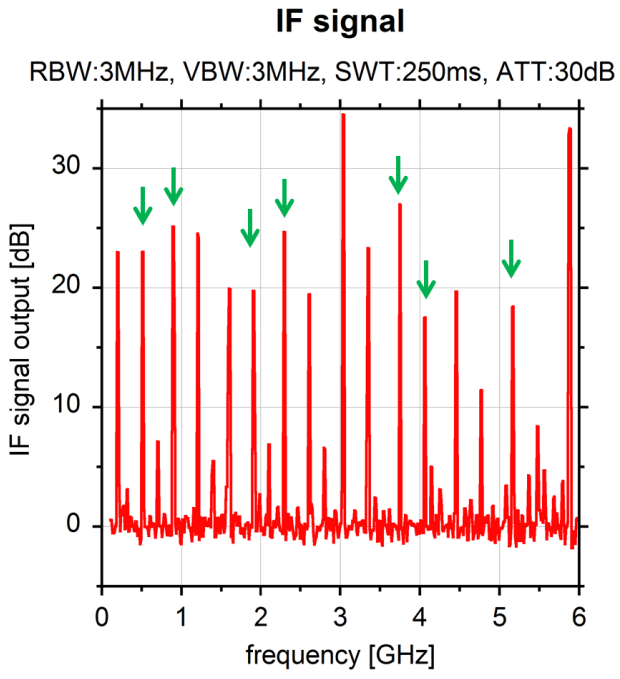

Fig. 4 Frequency spectrum of the IF signal, which is the microwave mixer output. The arrows indicate the utilized frequency components in the filter bank system.

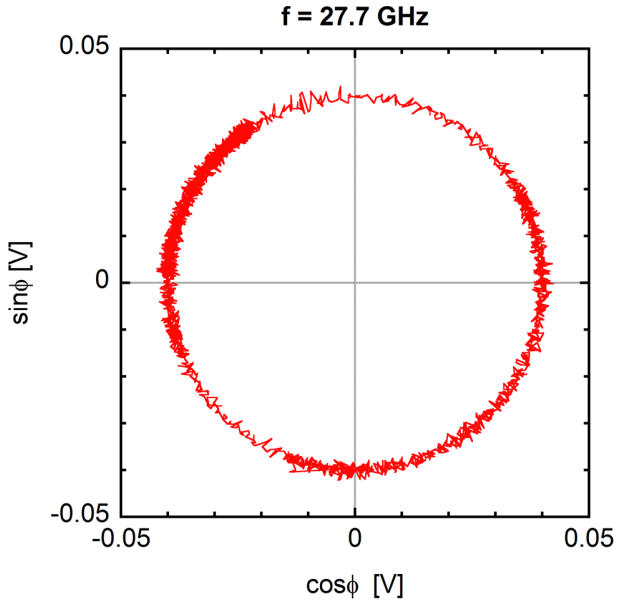

Fig. 5 Example of a phasor plot (IQ-plot) of the 27.7 GHz frequency component.

section described in Fig. 3. The IF signal is divided into eight signals by an 8-way splitter. Currently, a seven-channel filter bank system is employed. The center frequencies of the band pass filter are 0.53, 0.88, 1.95, 2.30, 3.70, 4.08, and 5.10 GHz with a 200 MHz bandwidth. Each individual wave passing through the band pass filter is fed to an IQ mixer that outputs two signals with in-phase and quadrature-phase. As shown in Fig. 5, the IQ output is in the form of a circle when a linear phase variation arises. This provides information regarding the phase variation caused by plasma fluctuation. Finally, the data of the filter bank system are acquired by an analog to digital converter (ADC) system with a 1 MHz sampling rate and 16-bit resolution. In addition, we attempted to apply the direct signal acquisition system described below.

3. System Performance

Profile measurement is one of the purposes of the present diagnostics. However, the observation position is affected by the plasma condition such as the electron density and magnetic field. To obtain the radial scattering position and the perpendicular wave number $k_\perp$, the LHDGAUSS three-dimensional beam tracing code [19] was used. Figure 6(a) shows an example of the beam trace of a 36 GHz probe beam. The beam is launched from the lower right side, which is the outboard side in the horizontal cross section of the LHD, and reflected near the cut-off position of $\rho = 0.8$. The LHDGAUSS code calculates the perpendicular wave number $k_\perp$ to the magnetic field at each point of the ray trajectory from the plasma edge to the turning point. The measured wave number of the density fluctuation is then obtained at the ray turning point. In

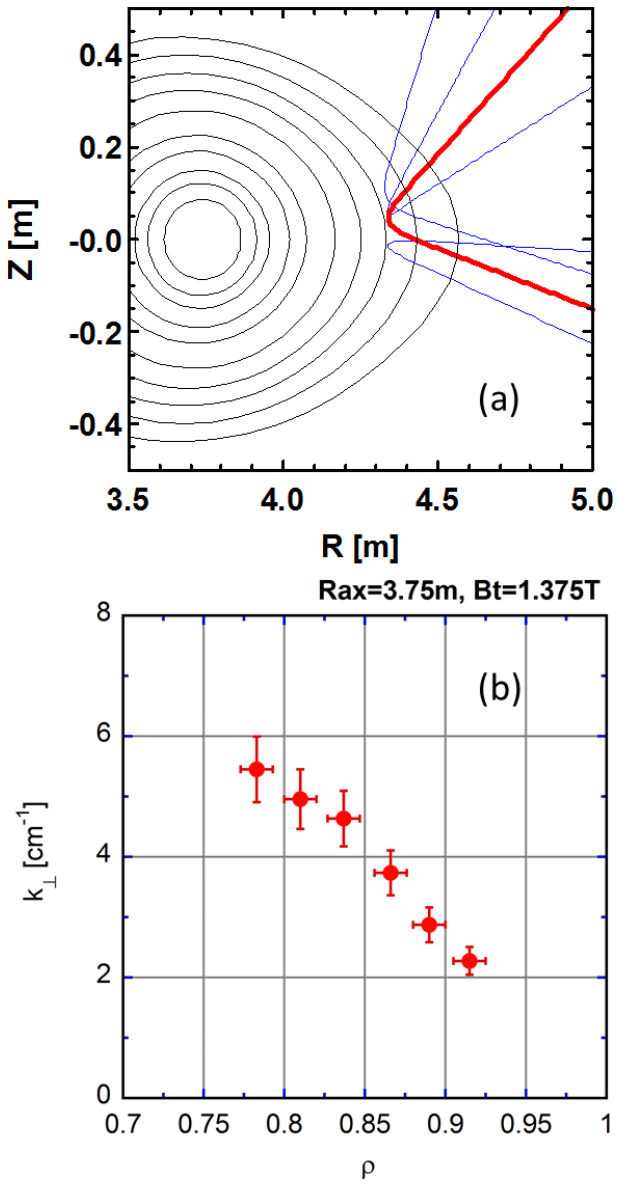

Fig. 6 (a) Example of the beam trace of a 36 GHz probe beam calculated by the LHDGAUSS code in the horizontal plasma cross section. Here, the red line shows the center ray and the beam width is expressed by the blue lines. (b) Example of the estimated wave numbers as a function of each scattered position.

Fig. 6(b), the radial dependence of the perpendicular wave number $k_\perp$ is shown for the case of six launching frequencies from 28 to 38 GHz. Of course, when the antenna angle, the plasma condition, and/or the utilized frequency are changed in the experiments, the measured wave number exhibits a wide variety that can be as high as 15 cm^{-1}.

Preliminary LHD plasma measurements were performed. Figure 7 illustrates the temporal evolution of the Doppler frequency spectra around the interruption of tangential neutral beam injection (t-NBI). In this figure, the mean frequency, which is calculated by the simple spectrum weighted mean technique [3], is indicated by the black line. This data is obtained under the condition that the magnetic axis position in the vacuum field is R_{ax} = 3.60 m, and the magnetic field strength is B_t = −2.75 T. During the time frame of interest, the perpendicular NBI sustains the plasma. Prior to the interruption of t-NBI, the electron density and the stored energy are kept nearly constant but the negative plasma current is increased. As can be seen, the most inner core channel of 31.95 GHz shows that the Doppler shifted frequency is decreasing toward the negative frequency direction during t-NBI. After t-NBI interruption, the Doppler frequency is increasingly turned. On the other hand, the outer channels show slightly delayed responses. These frequency shifts correspond with the poloidal flow at each position because the density profile is nearly steady over this period. Poloidal flow and parallel flow are related to each other through the medium of the electric field. Similar fast response against tangential NBI has also been observed in tokamaks [5, 8]. In addition, the stored energy decreases just after the interruption but the plasma current responds with a finite delay. It may be that the heating process is responding quickly to the power input, but the rotational torque is responding slowly. In addition, there are varieties of the Doppler shift frequency response at each channel. It may be shown that the poloidal flow has a fine structure. However, when the estimated Doppler shift peak frequency has a small value, it is often affected by the zero frequency components (that is, spurious carrier wave components) and the error of estimation is relatively increased. Therefore, this diagnostics yields an interesting plasma feature.

4. Direct Signal Acquisition

Now, we describe the preliminary test results of direct signal acquisition in an LHD plasma experiment. The direct signal acquisition is one of the effective developments for adding more channels to the multi-channel system because the current observation channel number is limited by the number of filter banks. The frequency comb reflectometer presently has around 20 frequency components. If the signal is acquired directly, it might obtain all of the frequency components, which provides much more spatio-temporal information. Another problem is the distance of separation between the data acquisition and the microwave system that is installed in LHD experimental room, which is a distance of approximately 100 m. For a solution, we utilize optical fiber transmission with an electro-optical converter, whose effective frequency range is presently up to 3 GHz. The reduced IF frequency is also useful at this point. This additional system is illustrated in Fig. 3. Then, a high frequency sampling rate digital oscilloscope (LeCroy: WaveMaster 820Zi-A [20]) is used for direct signal acquisition. Its bandwidth is 20 GHz and the sampling rate is 80 GS/s which is sufficient to demonstrate direct signal acquisition.

Figure 8 shows an example of the frequency spectra

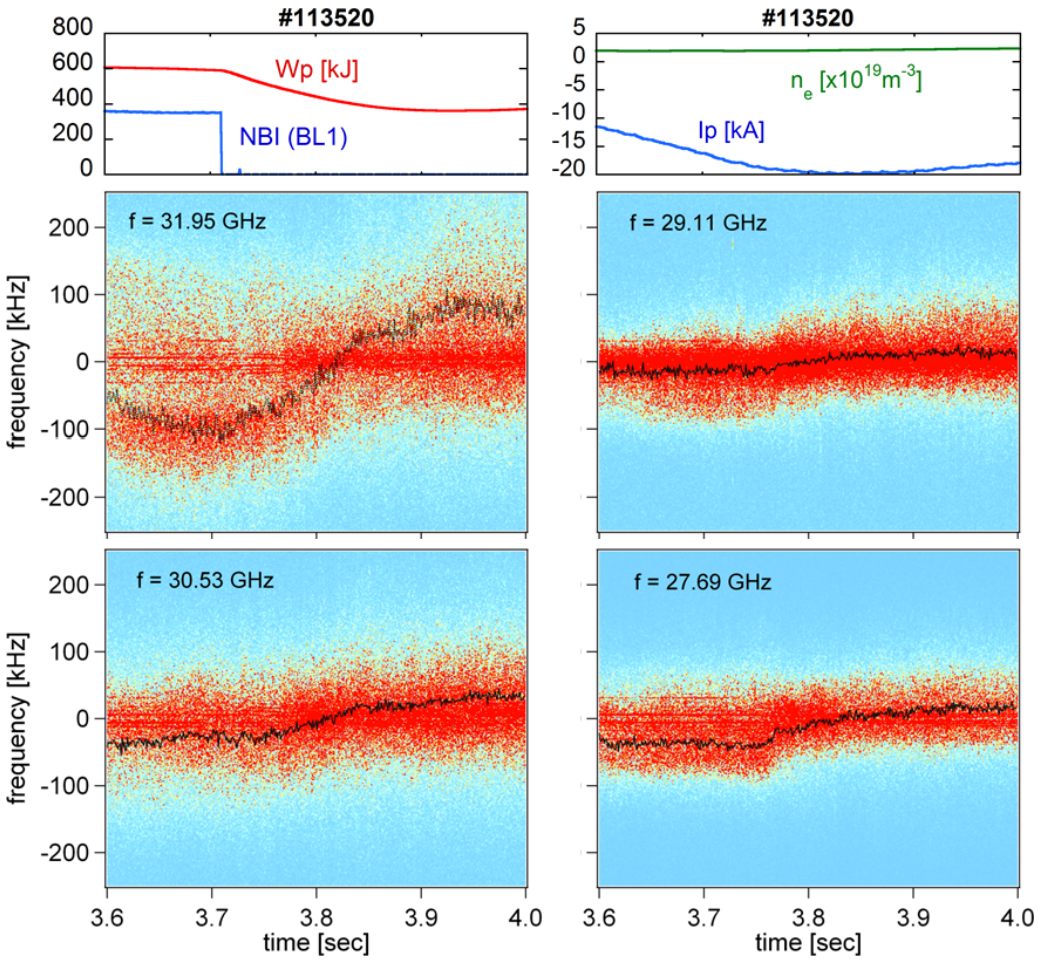

Fig. 7 Temporal evolution of complex frequency spectra as a response of neutral beam injection. The estimated frequency peak of the Doppler shift is inset with a black line indicative of the mean frequency. The stored energy (Wp), the line-averaged electron density (n_e), and the plasma current (Ip) are also plotted (at top).

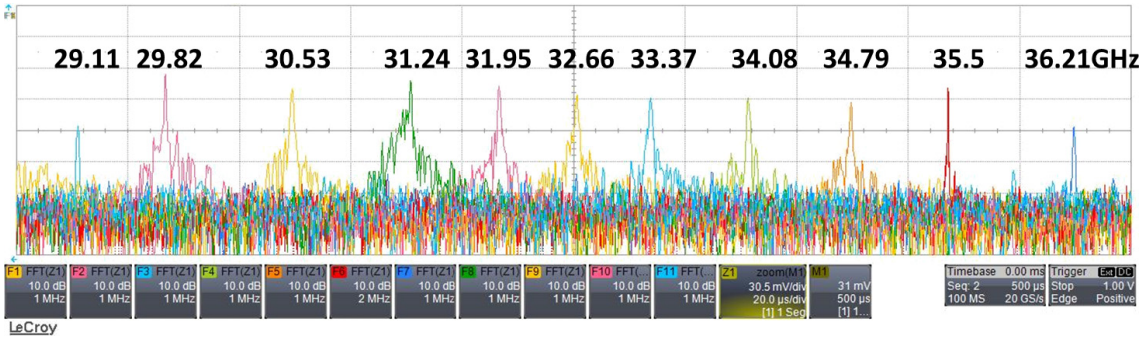

Fig. 8 Example of each frequency comb component scattered back from the corresponding layer in an LHD plasma. In this figure (oscilloscope capture), the frequency spectra are plotted overlaid one upon another. The horizontal axis indicates the frequency (1 MHz/div) and the vertical axis shows the power (10 dB/div).

obtained by the oscilloscope on-board analysis and display software. Here, 500 μs of stored data is used for making this graph. The frequency combs are all overlayed in a single viewer. Using this tool, several Doppler shifted frequency comb components are observed simultaneously. Note that this capture is a rough analysis. We subsequently calculated 100 MWords (that is 5 ms) of stored data for extracting each Doppler shift frequency from the digital frequency analysis mentioned above. The data size is limited by the computer memory size, which affects the resolution. The obtained radial profile of the poloidal velocity is shown in Fig. 9. Here, charge exchange spectroscopy

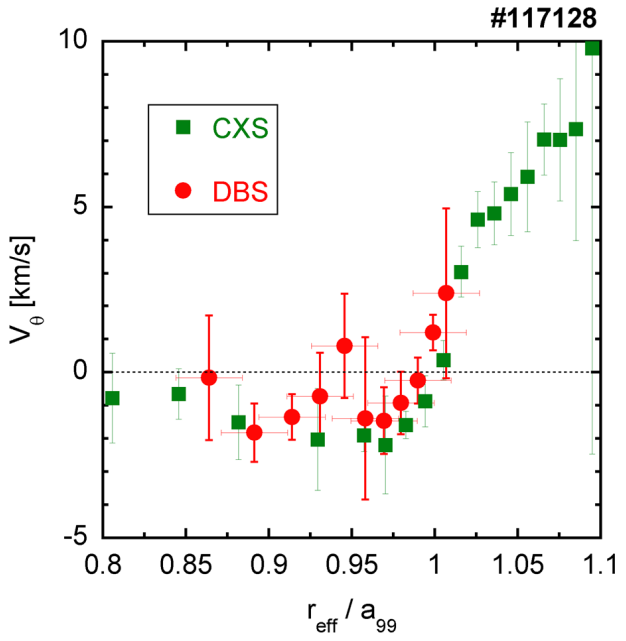

Fig. 9 Radial profiles of the poloidal velocity measured by the multi-channel Doppler reflectometer (DBS: red circles) and charge exchange spectroscopy (CXS: green squares).

(CXS) [21] data is also plotted and they are nearly in agreement. Therefore, it is determined that direct signal acquisition can be utilized.

Acknowledgments

The present study was supported in part by KAKENHI (Nos. 26630474, 25289342, 23244113, 23360414, 22360394, 22017007, and 21224014), by a Grant-in-Aid from the NIFS LHD project under the auspices of the NIFS Collaboration Research Program, and by the collaboration programs of the RIAM of Kyushu University and the Asada Science foundation. Additional support was provided by Japan/U.S. Cooperation in Fusion Research and Development.

[1] M. Hirsch *et al.*, Plasma Phys. Control. Fusion **43**, 1641 (2001).
[2] V.V. Bulanin *et al.*, Plasma Phys. Rep. **26**, 813 (2000).
[3] G.D. Conway *et al.*, Plasma Phys. Control. Fusion **46**, 951 (2004).
[4] J. Schirmer *et al.*, Plasma Phys. Control. Fusion **49**, 1019 (2007).
[5] G.D. Conway *et al.*, Nucl. Fusion **46**, S799 (2006).
[6] P. Hennequin *et al.*, Rev. Sci. Instrum. **75**, 3881 (2004).
[7] P. Hennequin *et al.*, Nucl. Fusion **46**, S771 (2006).
[8] J.C. Hillesheim *et al.*, Rev. Sci. Instrum. **80**, 083507 (2009).
[9] W.A. Peebles *et al.*, Rev. Sci. Instrum. **81**, 10D902 (2010).
[10] N. Oyama *et al.*, Plasma Fusion Res. **6**, 1402014 (2011).
[11] M. Hirsch *et al.*, Rev. Sci. Instrum. **72**, 324 (2001).
[12] T. Happel *et al.*, Rev. Sci. Instrum. **80**, 073502 (2009).
[13] T. Tokuzawa *et al.*, Rev. Sci. Instrum. **83**, 10E322 (2012).
[14] J.L. Hall and T.W. Hänsch, in 2005 Nobel Prize in Physics.
[15] T. Yasui *et al.*, Appl. Phys. Lett. **87**, 061101 (2005).
[16] S.H. Pepper and K. Schoen, "Microwaves and RF", October 2005, http://www.mwrf.com/articles/articleid/11224/11224.html
[17] Picosecond Pulse Labs, Boulder, CO, Microwave Journal, May 2006, http://www.picosecond.com/objects/mwj_reprint.pdf
[18] Y. Yokota *et al.*, Rev. Sci. Instrum. **79**, 056106 (2008).
[19] S. Kubo *et al.*, "ECH Power Deposition Study in the Collisonless Plasma of LHD" in Proceedings of 11th Int. Congress on Plasma Physics (July 2002, Sydney, Australia) p.133 (2002).
[20] http://teledynelecroy.com/japan/products/scopes/wm8zi
[21] K. Ida *et al.*, Rev. Sci. Instrum. **71**, 2360 (2000).